Vietnam Journal of Science and Technology ***63*** *(3) (2025) 619-629*

doi:10.15625/2525-2518/19409

Evaluating dynamic tire pressure variations on uneven road surfaces

Huynh Van Quan

Campus in Ho Chi Minh City, University of Transport and Communications, No. 450-451 Le Van Viet Street, Tang Nhon Phu A Ward, Thu Duc City, Ho Chi Minh City, Viet Nam

Email: *quanhv_ph@utc.edu.vn*

Received: 13 November 2023; Accepted for publication: 7 May 2025

Abstract. In order to accommodate Vietnamese conditions, this paper presents a road profile model that combines the international roughness index (IRI) with the Gaussian white noise (GWN) function. The proposed model deviates from the cosine model and the original model by about 3.6 % and less than 0.1 %, respectively. This model serves as an excitation source for analyzing the dynamic interaction between vehicles and pavements. Employing the MATLAB-Simulink tool, numerical dynamic analyses of a quarter-car model (QCM) were conducted at various vehicle speeds and road surface conditions. When comparing dynamic and static conditions, the results indicated a difference of over 10 % in the tire pressure applied to the pavement. For example, the deviations were 9.9, 16.4, 26.3, and 38.3 % at 40 km/h with corresponding IRI values of 1.8, 3.0, 5.0, and 7.0.

Keywords: road profile, international roughness index, vehicle-pavement interaction, dynamic tire pressure, pavement design.

Classification numbers: 5.4.1, 5.4.2, 5.10.2.

1. INTRODUCTION

Road roughness increases vehicle vibrations and tire pressure on the pavement, leading to dynamic vehicle–pavement interaction, which affects passenger comfort. In Viet Nam, current pavement designs are based on a constant pressure of 0.6 MPa, as defined in standards 22TCN 211-06 [1] and TCCS 38:2022/TCBVN [2]. However, dynamic tire pressure due to surface irregularities is also an important factor to consider.

Several researchers have examined the effects of dynamic tire pressure caused by road surface irregularities. Finite element analyses using ABAQUS have been applied to simulate random loading on asphalt pavements [3], although these methods are computationally intensive. Experimental techniques have also been employed to measure pavement stress and strain under dynamic loads [4], offering high accuracy despite their complexity and cost. Additionally, lumped-parameter models have been used to explore pavement responses under dynamic conditions [5 - 14]. In the context of Viet Nam, however, further investigation remains necessary to adapt and refine these approaches for practical application.

Synthetic random functions such as sine [15], cosine [11, 13, 16], or exponential [12, 17] have been widely used to generate road profiles in dynamic vehicle-pavement analysis, with the cosine function being the most common. Although vehicle speed has been considered in some cosine-based models, its influence remains insufficiently demonstrated. While ISO profiles use PSD to describe surface conditions, Viet Nam relies on IRI values. Recent studies [3, 14] have proposed models incorporating speed, randomness, and roughness for excitation.

To analyze dynamic vehicle-pavement interaction, various models have been used, including quarter-car [3, 5, 9, 16, 18], half-car [7, 8, 10, 17], and plane models [19, 20]. Among them, QCM is preferred for its efficiency in simulating uniform linear motion [3]. In addition, three-dimensional simulations based on the finite element method [21, 22] and full-scale vehicle experiments [23 - 25] have also been conducted.

As discussed, road roughness influences vehicle dynamics, leading to passenger discomfort, cargo instability, and increased tire pressure on the pavement. This study proposes a road profile function based on IRI data in Viet Nam and uses MATLAB-Simulink for numerical simulation. The focus is on the relationship between bus speed, road condition, and dynamic tire pressure.

2. PROPOSING A ROAD PROFILE MODEL

2.1. Description

In the time domain, the road profile $h(t)$ is defined by the differential equation [3, 14]:

$$\dot{h}(t) = -2\pi \cdot n_{00} \cdot u \cdot h(t) + 2\pi \cdot n_0 \sqrt{G_q(n_0) \cdot u} \cdot w(t) \quad (1)$$

where $n_{00} = 0.01$, u is vehicle speed, $n_0 = 0.1$ m^{-1} is the reference spatial frequency, $G_q(n_0)$ is the roughness coefficient (classified from A to H), and $w(t)$ is Gaussian white noise (GWN) with a PSD of 1.0 and mean of 0.0.

According to [13], the relationship between road PSD and IRI is given by:

$$G_q(n_0) = 1.63 \cdot K_0 \cdot IRI^2 \quad (2)$$

where $K_0 = 10^{-6}$ m^3. For example, the IRI from the mean $G_q(n_0)$ of class B is given by Eq. (3), with the full conversion table shown in Table 1.

$$IRI = \sqrt{\frac{G_q(n_0)}{1.63K_0}} = \sqrt{\frac{64 \cdot 10^{-6}}{1.63 \cdot 10^{-6}}} = 6.27. \quad (3)$$

Table 1. Conversion of $G_d(n_0)$ to IRI values.

Road class	***A***		***B***		***C***		***D***	
Value	$G_q(n_0)$ (10^{-6} m^3)	*IRI*	$G_q(n_0)$ (10^{-6} m^3)	*IRI*	$G_q(n_0)$ (10^{-6} m^3)	*IRI*	$G_q(n_0)$ (10^{-6} m^3)	*IRI*
Lower bound	8	2.22	32	4.43	128	8.86	512	17.72
Geometric mean	16	3.13	64	6.27	256	12.53	1024	25.06
Upper bound	32	4.43	128	8.86	512	17.72	2048	35.45

The road profile function derived from Eqs. (1) - (2) is:

$$\dot{h}(t) = -2\pi \cdot n_{00} \cdot u \cdot h(t) + 2\pi \cdot n_0 \sqrt{1.63 \cdot K_0 \cdot (IRI)^2 \cdot u} \cdot w(t) \quad (4)$$

This function combines IRI, vehicle speed, and GWN noise to simulate vehicle–pavement interaction, as discussed in the following sections.

2.2. Simulation

The simulation uses MATLAB-Simulink with the Band-Limited White Noise Block to simulate the GWN function, which has a mean value of 0.0 and a PSD of 1.0. Figure 1 shows the time-domain wave signal. Figure 2a shows the simulation of Eq. (4) using the GWN block, while Fig. 2b presents a similar simulation of Eq. (1) from [14]. Table 2 provides the data used to validate both road profile models.

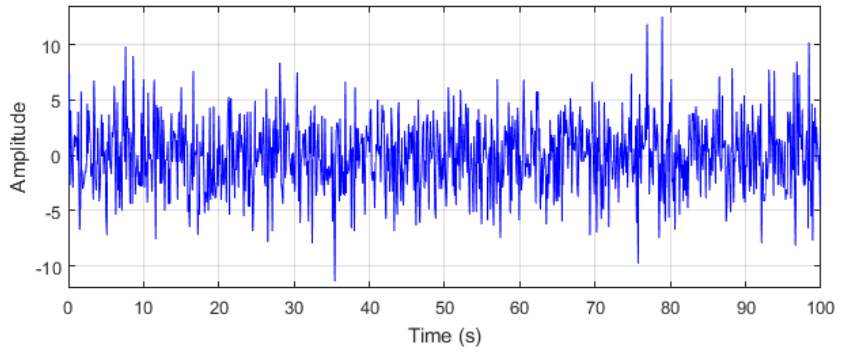

Figure 1. Waveform signal of GWN function over time.

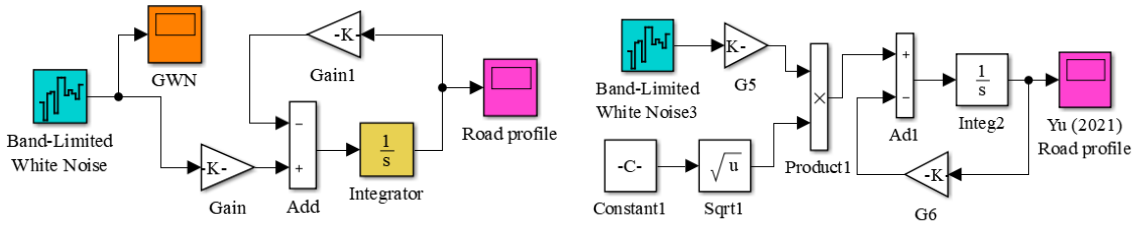

(a) Present simulation. (b) Simulation of [14].

Figure 2. MATLAB Simulink diagram for road profile simulations.

Table 2. Basic parameters of road profile [3, 14].

Parameter	K_0 (m^3)	n_0 (m^{-1})	n_{00}	u (km/h)	T (s)	B (m)	L (m)	Δn	N
Value	10^{-6}	0.1	0.01	40	100	0.25	1000	10^{-3}	4×10^3

Figures 3 and 4 show the simulated road profiles for class B and IRI values of 2.0 - 2.5 per TCVN 8865:2011 [27]. Table 3 compares the highest values from the proposed and cosine models [16]; errors are minimal-below 0.1 % for class B (due to rounding) and around 3.6 % for new road surfaces. The proposed model is used in subsequent dynamic analyses.

Table 3. The highest $h(t)$ value that each model could produce.

No.	IRI value	Reference (mm)		Proposal (mm)	Error (%)
1	3.13 (Class A)	Original model	21.55	21.53	0.09
2	6.27 (Class B)		43.10	43.13	0.07
3	12.53 (Class C)		86.21	86.19	0.02
5	2.0	Cosine model [16]	14.27	13.76	3.57
6	2.2		15.70	15.13	3.63
7	2.5		17.84	17.20	3.59

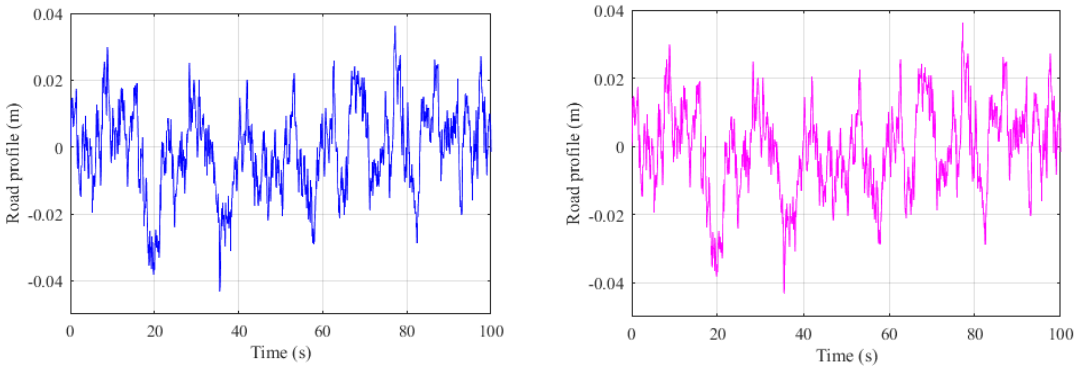

(a) The result of a proposal. (b) The result of original model.

Figure 3. Class B-road profiles.

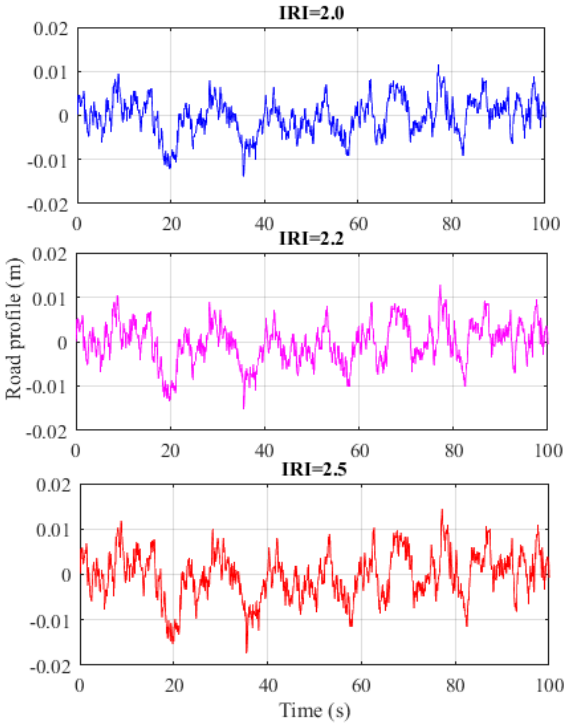

Figure 4. Road profiles with different IRI values of TCVN 8865:2011.

3. DYNAMIC TIRE PRESSURE ON PAVEMENT

3.1. Mathematical formulation

This study uses the QCM system (Fig. 5) for dynamic vehicle-pavement analysis. The sprung mass (m_s) is the vehicle body mass supported by one wheel, while the unsprung mass (m_u) includes the wheel, tire, and half the axle or suspension. The QCM has two DOFs representing wheel mass (z_u) and body mass (z_s). Suspension spring and damping rates are k_s and C_s, tire spring rate is k_t, and h represents the random road profile along the x direction.

$$\begin{cases} \frac{d}{dt}\left(\frac{\partial T}{\partial \dot{z}_s}\right) - \frac{\partial T}{\partial z_s} = Q_s \\ \frac{d}{dt}\left(\frac{\partial T}{\partial \dot{z}_u}\right) - \frac{\partial T}{\partial z_u} = Q_u \end{cases} \tag{5}$$

The equations of differential motion produce the following when the lumped rigid bodies in Eq. (5) are subjected to the Lagrange method [7, 16]:

$$\begin{cases} m_s\ddot{z}_s = -c_s(\dot{z}_s - \dot{z}_u) - k_s(z_s - z_u) \\ m_u\ddot{z}_u = c_s(\dot{z}_s - \dot{z}_u) + k_s(z_s - z_u) - k_t(z_u - h) \end{cases} \tag{6}$$

and expressed in vector forms

$$\boldsymbol{M\ddot{z}} = \boldsymbol{C\dot{z}} + \boldsymbol{Kz} + \boldsymbol{B} \tag{7}$$

where $\boldsymbol{z} = \begin{Bmatrix} z_s \\ z_u \end{Bmatrix}$, $\boldsymbol{M} = \begin{bmatrix} m_s & 0 \\ 0 & m_u \end{bmatrix}$, $\boldsymbol{C} = \begin{bmatrix} -c_s & c_s \\ c_s & -c_s \end{bmatrix}$, $\boldsymbol{K} = \begin{bmatrix} -k_s & k_s \\ k_s & -k_s - k_t \end{bmatrix}$, $\boldsymbol{B} = \begin{Bmatrix} 0 \\ k_t h \end{Bmatrix}$, h is the road profile, as stated in Eq. (4).

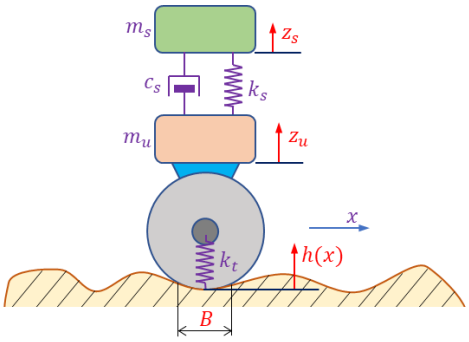

Figure 5. Quarter-car model [18].

The additional dynamic load of the tire on the pavement (F_d) brought on by car vibration and the static load of the car (F_s) are calculated using Eqs. (8) and (9):

$$F_d = k_t(z_u - h) \tag{8}$$

$$F_s = (m_s + m_u)g \tag{9}$$

where z_u is the tire's vertical displacement from Eq. (7), and $g = 9.81$ m/s².

The vehicle random dynamic load F_t, which is composed of the car static load F_s and the additional dynamic load F_d, is then applied to the road surface as follows:

$$F_t = F_d + F_s = k_t(z_u - h) + (m_s + m_u)g \quad (10)$$

Uneven road surfaces cause vibrations in the QCM system, increasing the dynamic vertical loads on the pavement, reflected as tire dynamic pressure. Studies [28, 29] show the wheel-road contact area is elliptical, modeled as a polygon with two semicircles and a rectangle of dimensions L and $0.6L$, also used in recent research [30]. Here, the contact area is calculated as:

$$A = \frac{3.14(0.6L)^2}{4} + 0.4L \cdot 0.6L = 0.5226L^2 \quad (11)$$

It is possible to determine the static pressure and instantaneous dynamic pressure of tires on pavement using Eqs. (12) and (13), respectively.

$$q_s = \frac{F_s}{A} = \frac{(m_s+m_u)g}{A} \quad (12)$$

$$q_t = \frac{F_t}{A} = \frac{k_t(z_u-h)+(m_s+m_u)g}{A} = q_s + \frac{F_d}{A} \quad (13)$$

In this paper, we propose to use Eq. (14) instead of Eq. (13) to calculate the average dynamic pressure on the survey distance. The dynamic load coefficient (DLC) represents the variation of dynamic loads and is defined by Eq. (15) [6, 9, 14]. DLC is determined by the magnitude of the dynamic variation of axle load for a given combination of road surface roughness and vehicle speed [10].

$$q_{d,a} = (1 + DLC) \cdot \frac{F_s}{A} = (1 + DLC) \cdot \frac{(m_s+m_u)g}{A} = (1 + DLC)q_s \quad (14)$$

$$DLC = \frac{1}{F_s}\sqrt{\frac{\sum_1^N (F_{t_i}-F_s)^2}{N-1}} \cdot 100\% \quad (15)$$

where N is the total number of steps and F_{t_i} is the dynamic force at step i.

However, using Eq. (16), we can also see that the DLC is equal to the difference between the average dynamic and static pressures, and this value is independent of contact area A.

$$\frac{q_{d,a}-q_s}{q_s} = \frac{(1+DLC)F_s-F_s}{F_s} = DLC \quad (16)$$

Therefore, it can be clearly seen that the determination of DLC values in the dynamic analysis of vehicle-pavement interaction are extremely important.

3.2. Numerical calculations

This section numerically investigates the bus QCM using the parameters in Table 4. Numerical modeling used tire footprints of 20×29 cm [30], giving a contact area $A = 29 \cdot 20 = 580$ cm^2. The QCM contact length $L = 25$ cm [18] yields $A = 551$ cm^2 from Eq. (11). This paper uses $A = 551$ cm^2 for consistency, with only a 5 % difference between models. Static tire pressure on pavement, calculated by Eq. (12), is $\frac{(4000+550)\cdot 9.81}{551} = 81.01$ N/cm^2.

Table 4. Bus QCM's dynamic parameters [11].

Parameter	m_s (kg)	m_u (kg)	k_s (10^4 N/m)	c_s (10^4 Ns/m)	k_t (10^6 N/m)
Value	4000	550	32	1.0	1.7

Row 1 in Table 5 shows A1-high class road quality based on TCVN 8865:2011 IRI values. This study uses four IRI values (1.8, 3.0, 5.0, 7.0) representing various surface conditions (row 2, Table 5). Corresponding constant bus speeds are analyzed; for example, IRI = 1.8 (good condition) matches speeds of 100, 60, 50, and 40 km/h (row 3). Distances traveled in 100 seconds (row 4) exceed the 200 m minimum per TCVN 8865:2011. Figure 6 shows road profiles at IRI = 1.8 and different speeds using the proposed Simulink model.

Table 5. Suggestions for IRI values and bus speeds.

No.	Surface condition	Good	Fair	Poor	Very poor
1	IRI range [27]	$IRI < 2$	$2 \leq IRI < 4$	$4 \leq IRI < 6$	$6 \leq IRI < 8$
2	Representative IRI	1.8	3.0	5.0	7.0
3	Bus speed (km/h)	{100, 80, 60, 40}	{80, 60, 50, 40}	{60, 50, 40, 30}	{40, 30, 20, 10}
4	Distance (S_u) (km)	$S_{100} = 2.78, S_{80} = 2.22, S_{60} = 1.67, S_{50} = 1.39,$ $S_{40} = 1.11, S_{30} = 0.83, S_{20} = 2.78, S_{10} = 0.28$			

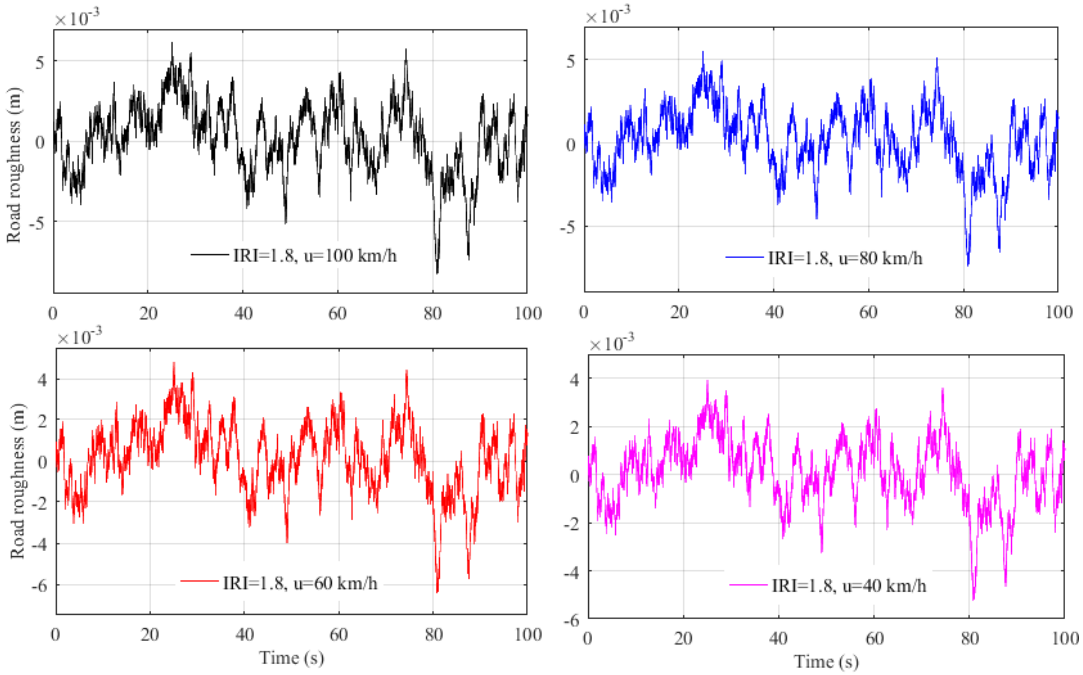

Figure 6. Road profiles with an IRI of 1.8 and at various speeds.

Figure 7 illustrates the MATLAB-Simulink simulation of Eq. (7) over 100 s with a 0.01 s step using Runge-Kutta integration. The input road profile comes from the Simulink analysis in Fig. 2a. Vertical vibrations (Fig. 8) and results (Table 6) are obtained from this simulation.

Rows 2 and 10 in Table 6 show that max road roughness $h_{max}(t)$ increases with IRI and vehicle speed. For a bus at 40 km/h, $h_{max}(t)$ rises with IRI values of 5.25, 8.76, 14.59, and 20.43 mm; at IRI = 1.8, $h_{max}(t)$ increases from 5.25 to 8.31 mm as speed rises from 40 to 100 km/h. Similar trends appear in z_u and DLC (rows 3, 4, 11, 12). Faster speeds on rougher roads increase vertical vibrations and reflect poorer road profiles, consistent with theory [31, 32].

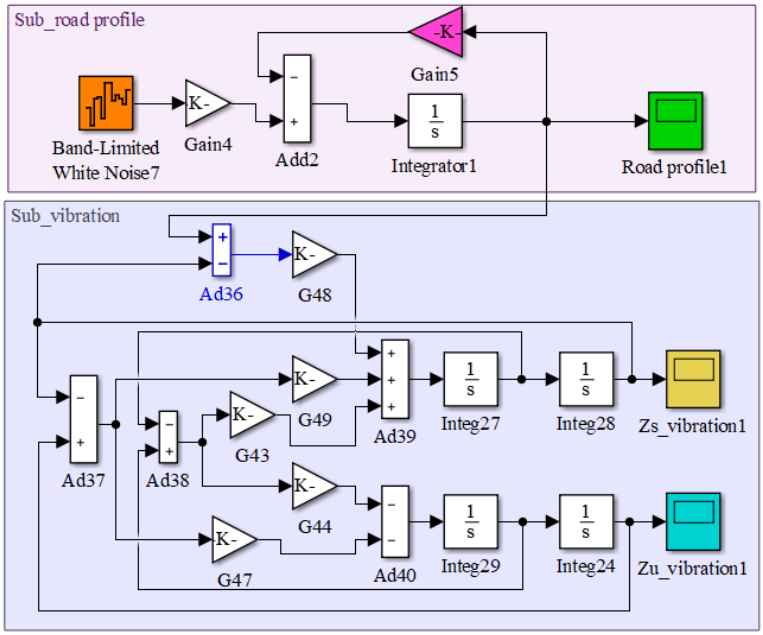

Figure 7. Simulink diagram for Eq. (7).

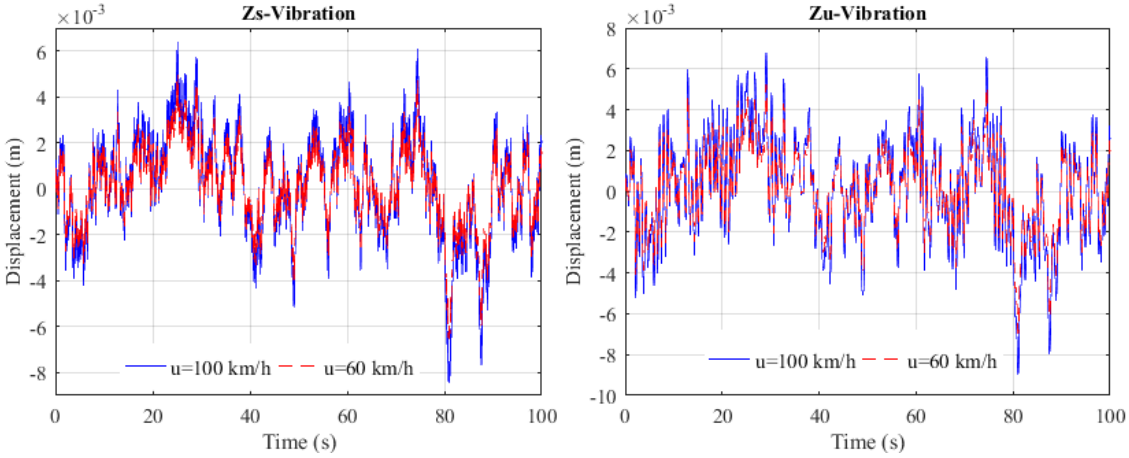

Figure 8. In case of IRI = 1.8, 100-s vibrations of the suspension and axle DOFs.

Dynamic pressure measures instantaneous max values, but average dynamic pressure over 100 s (hundreds of meters) should be used in calculations. Rows 5-6 and 13-14 show instantaneous and average dynamic pressures exceed static pressure. Differences between average and instantaneous pressures (rows 7, 15) range from 0.58 to 2.50 N/cm². For IRI = 1.8 at 100 km/h, average dynamic pressure is 93.65 N/cm², 15.6 % higher than static; at 40 km/h, deviation drops to 9.9 %. At 40 km/h, higher IRI (3.0, 5.0, 7.0) causes larger deviations (16.4 %, 26.3 %, 38.3 %).

Table 6. Process of computing dynamic pressure numerically.

No.	**IRI value**	**1.8**				**3.0**			
1	**Speed (u)**	**100**	**80**	**60**	**40**	**80**	**60**	**50**	40
2	h_{max} (mm)	8.31	7.43	6.44	5.25	9.21	10.72	9.79	8.76
3	z_u^{max} (mm)	8.96	8.02	6.94	5.70	13.36	11.57	10.56	9.45
4	DLC (%)	15.58	13.93	12.07	9.85	23.22	20.11	18.36	16.42
5	q_t^{max} (N/cm^2)	94.55	93.12	91.50	89.57	101.20	98.49	96.96	95.28
6	$q_{d,a}$ (N/cm^2)	93.63	92.30	90.78	88.99	99.82	97.30	95.88	94.31
7	$q_t^{max} - q_{d,a}$ (N/cm^2)	0.92	0.82	0.72	0.58	1.38	1.19	1.08	0.97
8	**IRI value**	**5.0**				**7.0**			
9	**Speed (u)**	**60**	**50**	**40**	**30**	**40**	**30**	**20**	**10**
10	h_{max} (mm)	17.87	16.32	14.59	12.64	20.43	17.69	14.45	10.22
11	z_u^{max} (mm)	19.29	17.61	15.75	13.64	22.05	19.09	15.59	11.02
12	DLC (%)	33.52	30.60	27.37	23.70	38.32	33.18	27.09	19.16
13	q_t^{max}(N/cm^2)	110.10	107.60	104.80	101.60	114.30	109.80	104.60	97.66
14	$q_{d,a}$ (N/cm^2)	108.20	105.8	102.30	100.20	112.00	107.90	103.00	96.53
15	$q_t^{max} - q_{d,a}$ (N/cm^2)	1.90	1.80	2.50	1.40	2.30	1.90	1.60	1.13

4. CONCLUSIONS

In this study, a road profile model combining the GWN function with IRI values (Eq. 4) were proposed, showing deviations of 3.6 % from a random cosine model and less than 0.1 % from the original model. Numerical simulations using a QCM in MATLAB-Simulink were performed to analyze vehicle-pavement interaction under various IRI levels (1.8, 3.0, 5.0, and 7.0) and bus speeds (10 - 100 km/h). The results emphasize the significance of DLC, which quantifies the difference between average dynamic and static pressures. At 40 km/h, pressure deviations reached 9.9, 16.4, 26.3, and 38.3 %, respectively. The use of average dynamic pressure via DLC is recommended in pavement design to improve load representation and structural accuracy. This approach supports compliance with Vietnam's 22TCN 211-06 and TCCS 38:2022/TCBVN specifications and contributes to the development of more reliable and realistic pavement structures.

Declaration of competing interest. The author declares that there are no known competing financial interests or personal relationships that could have appeared to influence the work reported in this paper.

REFERENCES

1. National Specification of Vietnam, 22TCN211-06 - Flexible Pavement Design-Specification and Guidelines, Vietnam Ministry of Transport, 2006 (in Vietnamese).
2. National Specification of Vietnam, TCCS38:2022/TCĐBVN - Specifications and Guidelines for Flexible Pavement Design on the Structural Number (SN), Vietnam Ministry of Transport, 2022 (in Vietnamese).
3. Ye Z., Miao Y., Zhang W., Wang L. - Effects of random non-uniform load on asphalt pavement dynamic response, International Journal of Pavement Research and Technology **14** (2020) 299-308. doi.org/10.1007/s42947-020-0147-0.

4. Hsing C. H., Siao J. H., Wang Y. M. - A study on the design depth of permeable road pavement through dynamic load experiment, Materials **15** (2022) 4391. doi.org/10.3390/ma15134391.
5. Loizos A., Plati C. - An alternative approach to pavement roughness evaluation, International Journal of Pavement Engineering **9** (2008) 69-78. doi.org/10.1080/10298430600949894.
6. Shi X. M., Cai C. S. - Simulation of dynamic effects of vehicles on pavement using a 3D interaction model, Journal of Transportation Engineering **135** (2009) 736-744. doi.org/10.1061/(ASCE)TE.1943-5436.0000045.
7. Barbosa R. S. -Vehicle dynamic response due to pavement roughness. Journal of the Brazilian Society of Mechanical Sciences and Engineering, **33** (2011) 302-307. doi.org/10.1590/S1678-58782011000300005.
8. Barbosa R. S. - Vehicle vibration response subjected to longwave measured pavement irregularity, Journal of Mechanical Engineering and Automation **2** (2012) 17-24. doi.org/10.5923/j.jmea.20120202.04.
9. Buhari R., Rohani M. M., Abdullah M. E. - Dynamic load coefficient of tyre forces from truck axles, Applied Mechanics and Materials **405** (2013) 1900-1911. doi.org/10.4028/www.scientific.net/AMM.405-408.1900.
10. Park D. W., Papagiannakis A. T., Kim I. T. - Analysis of dynamic vehicle loads using vehicle pavement interaction model, KSCE Journal of Civil Engineering **18** (2014) 2085-2092. doi.org/10.1007/s12205-014-0602-3.
11. Agostinacchio M., D. Ciampa, S. Olita. - The vibrations induced by surface irregularities in road pavements-A Matlab® approach, European Transport Research Review **6** (2014) 267-275. doi.org/10.1007/s12544-013-0127-8.
12. Zhao L. Y., Yang J. L., Chen L. X., Yu J. B., Mu G. - Proceedings of the 2nd 2016 International Conference on Sustainable Development, Atlantis Press, 2016, pp. 506-510.
13. Han F., Wang H., Dan D. H. - Proceedings of the Institution of Civil Engineers-Transport, Thomas Telford Ltd, 2019, pp. 221-232.
14. Yu X., Liu X., Wang X., Wang X., Wang Y. - Proceedings of the Institution of Mechanical Engineers, Part D: Journal of Automobile Engineering (2021) 2253-2264.
15. Ma K., Zhang Y., Zhen X. -Simulation of Pavement Random Excitation Based on Harmonic Superposition Method. International Journal of Scientific Advances, **2** (2021) 282-285. doi.org/10.51542/ijscia.v2i3.9.
16. Quan H. V., Canh T. M., Phuc L. V. -Vehicle model dynamic analysis under random excitation of uneven pavement as measured by the international roughness index. Transport and Communications Science Journal **74** (2023) 866-880. doi.org/10.47869/tcsj.74.8.2. (Vietnamese).
17. Guo L. X., Zhang L. P. - Vehicle vibration analysis in changeable speeds solved by pseudo excitation method, Mathematical Problems in Engineering 2010 (2010) 1-14. doi.org/10.1155/2010/802720.
18. Sidess A., Ravina A., Oged E. -A model for predicting the deterioration of the international roughness index. International Journal of Pavement Engineering **23** (2022) 1393-1403. doi.org/10.1080/10298436.2020.1804062.
19. Dang H. H. H., Son D. T., Hoang T. M. - Assessment of oscillating of light trucks under the impact of ISO road surface, Vietnam Mechanical Engineering Journal **4** (2017) 94-99.

20. Liu Y., Cui D. - Research on Road Roughness Based on NARX Neural Network, Mathematical Problems in Engineering 2021 (2021) 1-16. doi.org/10.1155/2021/9173870.
21. Lu Y., Yang S., Li S., Chen L. - Numerical and experimental investigation on stochastic dynamic load of a heavy-duty vehicle, Applied Mathematical Modelling **34** (2010) 2698-2710. doi.org/10.1016/j.apm.2009.12.006.
22. Liu P., Ravee V., Wang D., Oeser M. - Study of the influence of pavement unevenness on the mechanical response of asphalt pavement by means of the finite element method, Journal of Traffic and Transportation Engineering **5** (2018) 169-180. doi.org/ 10.1016/j.jtte.2017.12.001.
23. Kumaresh S. A., Aladdin M. F. - Proceedings of the AIP Conference, AIP Publishing (2019) 19-23. doi.org/10.19206/CE-2020-203.
24. Meram A., Shahriari M. - Evaluation of Whole-Body Vibration in Automobile on Routine Travel-A Case Study, Occupational and Environmental Safety and Health **202** (2019) 191-199. doi.org/10.1007/978-3-030-14730-3_21.
25. ShiW., Li M., Guo J., Zhai K. - Evaluation of road service performance based on human perception of vibration while driving vehicle, Journal of Advanced Transportation **2020** (2020) 1-8. doi.org/10.1155/2020/8825355.
26. International Organisation of Standardisation, ISO 8608:2016 - Mechanical vibration– Road surface profles–Reporting of measured data, Switzerland, 2016.
27. National Specification of Vietnam, TCVN8865:2011 - Method for measuring and assessment roughness by International Roughness Index, Vietnam Ministry of Transport, 2011 (in Vietnamese).
28. Association P. C. - Thickness design for concrete pavements, Skokie, IL: Portland Cement Association, 1966.
29. Yoder E. J., Witczak M. W. - Principles of pavement design. Hoboken, NJ, Wiley, 1975.
30. Assogba O. C., Tan Y., Sun Z., Lushinga N., Bin Z. - Effect of vehicle speed and overload on dynamic response of semi-rigid base asphalt pavement, Road Materials and Pavement Design **22** (2021) 572-602.doi.org/10.1080/14680629.2019.1614970.
31. Gillispie T. D., Karamihas S. M., Sayers M. W., Nasim M. A., Hansen W., Ehsan N., Cebon D. - Effect of heavy vehicle characteristics on pavement response and performance, Transportation Research Board NCHRP, Washington DC, 1993.
32. Cole D. J., Cebon D. - Truck suspension design to minimize road damage, IMechE. J. Auto. Eng. **210** (1996) 95-107.doi.org/10.1243/PIME_PROC_1996_210_251_02.